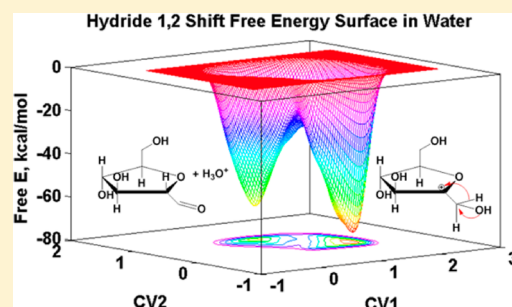


# Glucose Isomerization to Fructose from ab Initio Molecular Dynamics Simulations

Xianghong Qian\* and Xingfei Wei

Ralph E. Martin Department of Chemical Engineering, University of Arkansas, Fayetteville, Arkansas 72701, United States

**ABSTRACT:** Car–Parrinello molecular dynamics simulations (CPMD) coupled with metadynamics (MTD) simulations were conducted to investigate glucose isomerization to fructose in acidic aqueous solution. Glucose to fructose isomerization is initiated by protonation of the C2-OH and the formation of a furanose aldehyde intermediate. Fructose is produced via a hydride transfer from C2 to C1 on the furanose aldehyde followed by the rehydration of the C2 carbocation. Hydride 1,2 shift to form a C2 carbocation is an energetically favorable process but the barrier is relatively high at around 35 kcal/mol. The final step during glucose to fructose isomerization involves the rehydration of the C2 carbocation with an estimated barrier of 25 kcal/mol from our CPMD-MTD simulations.



## I. INTRODUCTION

Cellulosic biomass represents an abundant renewable resource for the production of biobased products and biofuels. 5-Hydroxymethylfurfural (HMF) is a critical and versatile intermediate for converting biomass to liquid alkanes and many other value-added products. High HMF yields from fructose have been achieved if processed in dimethyl sulfoxide (DMSO), ionic liquids, or other mixed solvents using a biphasic reactor.<sup>1–7</sup> However, cost-effective conversion of glucose, the dominant biomass monomer sugar, to HMF remains a critical issue. This is largely due to the existence of multiple reaction pathways during glucose reactions leading to the formation of various byproduct.<sup>8,9</sup> Experimentally, it was found that glucose conversion and selectivity are especially sensitive to the type of catalysts present and the solvent media.<sup>3,5,7,10–18</sup> Possible glucose reactions during liquid phase processing include condensation, mutarotation, isomerization, and dehydration/degradation reactions.<sup>19–21</sup> During Brønsted acid-catalyzed glucose reactions, our previous simulation results show that protonation of one of the hydroxyl groups on the glucose ring or the ring O and the subsequent breakage of the C–O bond is the critical step.<sup>9,19–22</sup> Our recent calculations<sup>9,19–22</sup> demonstrate that the barriers for acid-catalyzed glucose reactions are largely solvent induced due to the competition for proton between the hydroxyl groups on glucose and the solvent molecules.

Glucose condensation reaction is initiated by protonation of C1-OH and the subsequent formation of a C1-carbocation, followed by the formation of a 1, $\alpha$  linked ether bond with the second glucose molecule with  $\alpha = 1–4$  and 6.<sup>19</sup> Glucose mutarotation involving interconversion between  $\alpha$ -D-glucose and  $\beta$ -D-glucose is initiated by the protonation of the ring O and opening of the ring structure followed by the rotation of the C1 carbon, and the reclosing of the ring structure. Our earlier results<sup>19</sup> show that glucose mutarotation is also possible in aqueous solution via the formation of a C1-carbocation

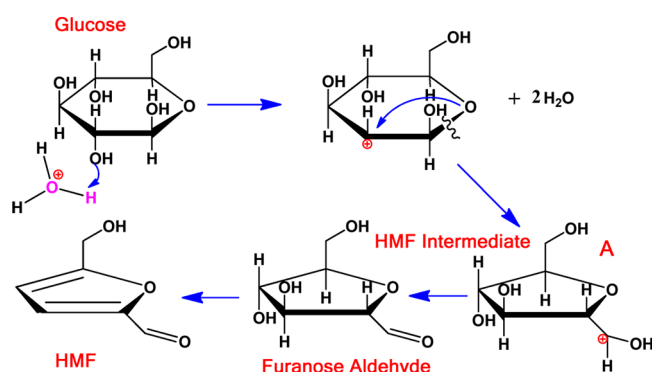
similar to the condensation reaction step, followed by the attack of the C1-carbocation by a solvent H<sub>2</sub>O molecule. The formation of either  $\alpha$ - or  $\beta$ -D-glucose conformer will depend on the position of the attack by the water molecule with respect to the glucose ring structure (above or below). Our earlier studies<sup>19,20</sup> have focused on the glucose condensation reactions to form disaccharides and the dehydration reaction to form HMF in acid catalyzed aqueous solutions. Here we will focus on the mechanisms involving glucose isomerization to fructose. Earlier studies in the literature<sup>7</sup> suggest that the first step during glucose to HMF dehydration is glucose isomerization to fructose transforming a pyranose ring to a furanose ring structure. However, there is not sufficient experimental and theoretical evidence to support this mechanism. Due to the similarity between xylose and glucose molecules, earlier investigations on xylose dehydration to furfural<sup>22</sup> could shed some light on glucose to HMF formation mechanism.

There are two mechanisms proposed in the literature for transforming the 6-member ring pyranose xylose molecule to the 5-member ring furanose furfural<sup>23–25</sup> for acid catalyzed sugar reactions. The mechanism proposed by Feather and Harris<sup>24,26,27</sup> involves a series of open chains. Initially the open chain form of the xylose aldose structure isomerizes to form a ketose structure. The open chain form of the ketose structure loses two water molecules via acid-catalyzed dehydration. Finally the open chain closes forming furfural. Based on experimental evidence, Antal and co-workers<sup>23,25</sup> proposed a cyclic mechanism involving direct transformation from a xylose pyranose ring to a furanose ring without opening the ring structure. A furanose aldehyde was proposed as an intermediate for the furfural formation. Since xylose dehydration to furfural is similar to glucose dehydration to HMF, Scheme 1 illustrates

Received: April 20, 2012

Revised: August 6, 2012

Published: August 15, 2012

Scheme 1. Cyclic Mechanism for Glucose Conversion to HMF<sup>a</sup>

<sup>a</sup>HMF formation is initiated by protonation of C2–OH followed by the breakage of a C2–O2 bond and the formation of a C2–O5 bond to form a furanose aldehyde intermediate. HMF is generated via further dehydration of this intermediate by losing two more water molecules on the furanose ring.

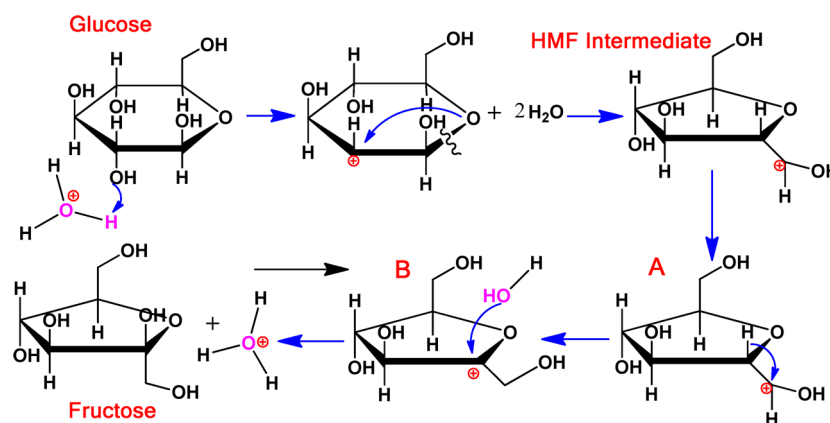
the glucose to HMF formation process, similar to the one suggested by Antal and co-workers for xylose to furfural formation.<sup>25</sup> HMF is formed by further dehydration of the furanose aldehyde intermediate removing two more water molecules. Further, Antal and co-workers<sup>23</sup> suggested that this furanose aldehyde is the intermediate leading to the formation of HMF from the initial reactant fructose via protonation at C1–OH. Our earlier *ab initio* molecular dynamics studies<sup>8,9,21,28</sup> using CPMD confirmed the mechanism proposed by Antal and co-workers for xylose to furfural formation. Further, our earlier results<sup>8,9,21,28</sup> show that protonation of C2–OH on  $\beta$ -D-glucose, the breakage of the C2–O2 bond and the formation of C2–O5 bond is the critical step for proton-catalyzed glucose to HMF conversion as shown in Scheme 1. Feather and Harris in their earlier publications<sup>24,26,27,29</sup> proposed the open chain mechanism for glucose reaction to form fructose and HMF based mostly on proton exchange experiments. A hydride transfer from C2 to C1 was found and used as supporting evidence for the open chain mechanism during the aldose to ketose transformation process. The cyclic mechanism for glucose transformation does not contradict the hydride C2 to C1 transfer process. Our results indicate that fructose is

generated via hydride C2 to C1 transfer from the furanose aldehyde intermediate formed via the cyclic mechanism as shown in Scheme 2. The details of glucose isomerization to fructose and hydride C2 to C1 transfer will be discussed here. As solvent plays a critical role in sugar reactions, the energetics and the barriers associated with the hydride transfer in the presence and absence of solvent water are determined. In addition, energetics associated with nucleophilic attack by H<sub>2</sub>O on the C2 carbocation leading to the formation of fructose is also calculated.

Scheme 2 shows that fructose could be produced through a 1,2 hydride transfer once the furanose intermediate A has formed. During the breakage of the C2–O2 bond and the formation of the C2–O5 bond, the C1–O5 bond also simultaneously breaks leaving a C1 carbocation outside the 5-member ring structure. The H atom on C2 could be transferred to C1 to form a secondary carbocation on C2 which can be stabilized by the neighboring ring O. This is the so-called 1,2 hydride transfer process. Another H<sub>2</sub>O molecule attacks the C2 carbocation to form either  $\alpha$ - or  $\beta$ -D-fructose. Our proposed mechanism agrees with the available experimental literature demonstrating the isotope effects observed for 1,2 hydride transfer.<sup>24,26</sup> This 1,2 hydride shift does not occur at the beginning of the glucose isomerization to fructose, rather it is close to the end of the isomerization process.

## II. COMPUTATIONAL METHOD

Car–Parrinello molecular dynamics simulations (CPMD) have been applied successfully and extensively for investigating sugar reactions in our earlier studies.<sup>8,9,19–22,28</sup> Coupled with metadynamics (MTD),<sup>30,31</sup> the free energy surfaces (FES) for sugar condensation, mutarotation, and dehydration reactions in aqueous solutions were determined. MTD is designed to enhance the probabilities of the energy-barrier crossing events during a chemical reaction or process.<sup>30,31</sup> The MTD method is based on the ideas of extended Lagrangian<sup>30,32–34</sup> and coarse-grained non-Markovian dynamics,<sup>30</sup> which allows for very efficient exploration of the FES of the reactive system. CPMD–MTD allows for accelerated sampling of chemical reactions involving bond breaking and bond formation processes. This method assumes that several collective coordinates, which distinguish reactants from products, are able to characterize the reaction process. These collective coordinates (e.g., distances

Scheme 2. Schematics for Acid-Catalyzed Glucose Isomerization to Fructose via the Cyclic Mechanism<sup>a</sup>

<sup>a</sup>The conversion is initiated by the protonation of C2–OH and the formation of a 5-member ring furanose intermediate A, followed by a hydride 1,2 shift transforming intermediate A to B. Rehydration of intermediate B at the C2 carbocation by one H<sub>2</sub>O molecule produces a fructose isomer.

between atoms and coordination numbers) must include the relevant modes that cannot be sampled within the typical time scale of the *ab initio* MD simulations. More details of the method and parameters used for investigating FES of sugar reactions can be found in our earlier work.<sup>19,22</sup>

For our CPMD-MTD simulations, the Becke, Lee, Yang, and Parr (BLYP) functional was used to describe valence and semicore electrons.<sup>35,36</sup> The potentials exerted by the core electrons were approximated by the Goedecker pseudopotentials<sup>37</sup> which has been found to yield excellent properties for glucose, xylose, and their reactions in water.<sup>19,22</sup> An energy cut off of 80 Ry was used for the plane wave basis sets. More details on the parameters can also be found in our previous publications.<sup>19,22</sup> The MD simulations were carried out under NVT at 300 K with a Nose-Hoover chain thermostat.<sup>38–40</sup> In the gas phase, the system contains one glucose intermediate A. The simulation box has a dimension of  $20 \times 20 \times 20$  Å and was decoupled from its image by using the Hockney's method with an extra 4 Å added to each dimension of the simulation box.<sup>41</sup> For all of the calculations in solution, the periodic boundary condition was used. In pure water, the systems contain one glucose intermediate A or B which are both positively charged, one Cl<sup>−</sup> counterion, and 74 (intermediate A) or 76 (intermediate B) H<sub>2</sub>O molecules. The simulation box size has a dimension of  $15 \times 15 \times 15$  Å and a corresponding density of about 0.8 g/cm<sup>3</sup>. Ewald summation was used to integrate the long-range electrostatic interaction energies.

In order to determine the free energy surface and the barriers associated with the hydride 1,2 shift process, CPMD-MTD simulations were conducted for the H shift from C2 to C1 transforming glucose intermediate A to B as shown in Scheme 2. Two collective variables (CVs) were selected to determine the transfer energetics. CV1 is the coordination number (CN) between C1 and two H atoms (H1 and H2) whereas CV2 is the CN between C2 and the same two H atoms (H1 and H2). The simulations were conducted in vacuum and then in aqueous solution in order to understand the influence of solvent water on the transfer energetics. The choice of CVs should reflect the actual reaction coordinates and is critical in obtaining accurate reaction barriers. Artificially reducing the number of CVs will result in overestimating the reaction barrier. Here the two CVs chosen appear to be sufficient as they are directly associated with the hydride transfer process.

For the process of fructose formation by H<sub>2</sub>O molecule nucleophilic attack on C2 carbocation on intermediate B, two coordination type CVs were also chosen. CV1 is the CN between C2 and O (H<sub>2</sub>O) representing the C–O bond. CV2 is the CN between O and H for the H<sub>2</sub>O molecule representing the O–H bond. Simulations were conducted in aqueous solution only since the presence of water is necessary for the reaction.

### III. RESULTS AND DISCUSSION

**III.1. Hydride 1,2 Shift in Vacuum.** Figures 1 and 2 are the CV variations and trajectories respectively during the course of over 800 MTD sampling process for hydride 1,2 shift on intermediate A in vacuum. From Figure 1, it can be seen that the CN for CV1 (blue) representing the C1–H bond varies between 1 and 2 corresponding to hydride transfer before and after respectively. The CN for CV2 (red) representing C2–H bond fluctuates between 0 and 1 also corresponding to the hydride transfer process before and after. Further it can be seen that the hydride was transferred several times between C1 and

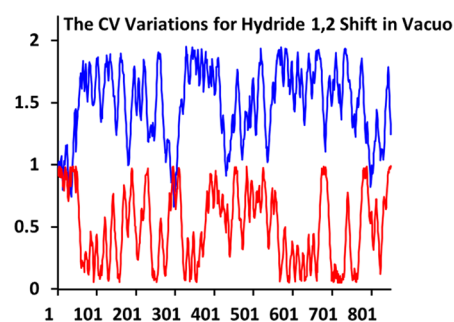


**Figure 1.** CV variations for H transfer from C2 to C1 transforming intermediate A to intermediate B during the course of CPMD-MTD simulations in the gas phase. The blue and red lines are the variations of the coordination numbers (CN) for the CV1 (C1–H, blue) and CV2 (C2–H, red).

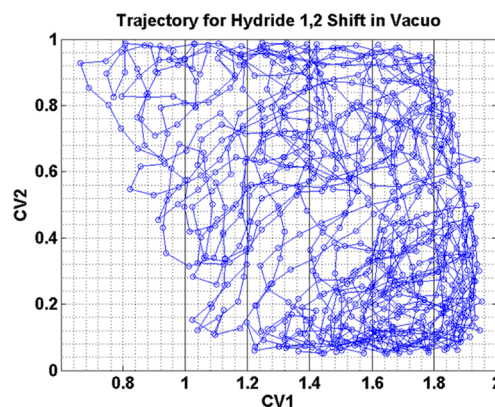


**Figure 2.** CV trajectories for CV1 (C1–H) and CV2 (C2–H) during the course of CPMD-MTD sampling process for hydride transfer from C2 to C1 transforming intermediate A to intermediate B in the gas phase.

C2 atoms indicating that the MTD sampling process is complete. Figure 2 shows the trajectories of the two CVs again indicating that there are sufficient samplings of the two CVs for hydride transfer during CPMD-MTD simulations.

Based on the repulsive potentials added to the reactant and product wells, the free energy surface (FES) is reconstructed. Figure 3 shows the free energy contour plot associated with the hydride transfer from C2–H to C1–H process during glucose

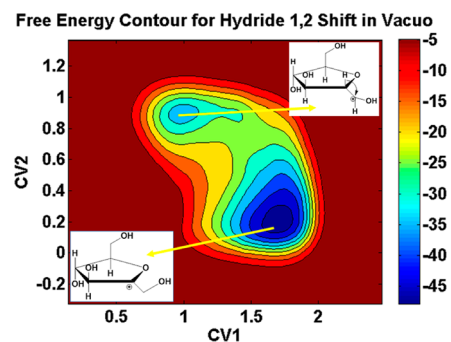


**Figure 3.** Free energy contour plot for hydride transfer from C2 to C1 on the furanose intermediate A during glucose isomerization to fructose in the gas phase. CV1 and CV2 represent the CNs between C1–H and C2–H, respectively. The isomerization is initiated by protonation of C2–OH and breakage of the C2–O2 bond and formation of the C2–O5 bond via the cyclic mechanism.



isomerization to fructose in the gas phase. Figure 4 exhibits the reconstructed three-dimensional FES. These free energy plots

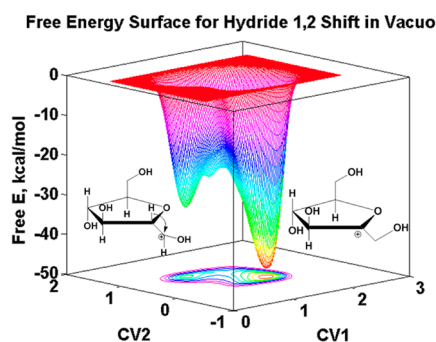


**Figure 4.** Reconstructed 3-D free energy surface for CV1 (C1–H) and CV2 (C2–H) representing hydride transfer from C2 to C1 process in the gas phase during glucose to fructose isomerization via the direct cyclic mechanism.

demonstrate that this hydride transfer process has a very low barrier in the gas phase with only about 5–7 kcal/mol. This is probably due to the relative higher stability of the secondary C2-carbocation compared to the primary C1-carbocation. The BLYP functional used here is known to underestimate the barrier for proton or hydride transfer slightly. As a result, the barrier obtained here is likely the lower bound of the activation energy. The initial structure (CV1  $\approx$  1 and CV2  $\approx$  1) before hydride transfer has a higher free energy than the final structure (CV1  $\approx$  1.7 and CV2  $\approx$  0.2) after the hydride transfer by about 15 kcal/mol. The transfer of the hydride from C2 to C1 appears to be a rather low barrier and energetically favorable process. However, In the presence of solvent water molecules, the energy barrier associated with hydride transfer from C2 to C1 will likely be different due to the instability of carbocation  $\text{—HC1}^+\text{—OH}$  on intermediate A in acidic aqueous solution. The water molecule could easily take the proton away thus neutralizing the positively charged intermediate A to form a furanose aldehyde with  $\text{—HC1=O}$  as was observed earlier in our CPMD simulations.<sup>8,9,19,20,22,28</sup> This is indeed the case when CPMD–MTD simulations were conducted for this hydride transfer process in aqueous solution which will be discussed in the next section.

**III.2. Hydride Transfer in Aqueous Solution.** Once the free energy surface and associated barrier were determined for the hydride transfer from C2 to C1 during glucose isomerization to fructose in the gas phase, CPMD-MTD simulations were carried out for this process in aqueous solution. The system includes one glucose intermediate A surrounded by 74 water molecules and one  $\text{Cl}^-$  counterion. Periodic boundary conditions were applied. The same two CVs as those in the gas phase were adopted for the sampling process in aqueous solution. CV1 is the CN between C1 and H and CV2 is the CN between C2 and H. Figures 5 and 6 show the variations of the coordination numbers and the trajectories of the two CVs respectively during over 900 MTD simulation steps. From Figure 5, it can be seen that the time evolution of the sampling dynamics is quite different from the corresponding one in the gas phase. However, the CV trajectories appear to be more or less the same as shown in Figure 6. Both CV1 and CV2 start at around 1 which indicates that H1 and H2 are bound to C1 and C2, respectively. During the CPMD-MTD simulations, CV1 fluctuates and slowly increases to 1.9 at around 300 MTD step,

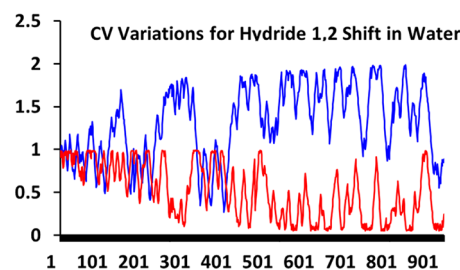


**Figure 5.** CV variations for hydride transfer from C2 to C1 transforming furanose glucose intermediate A to B during glucose to fructose isomerization during CPMD-MTD simulations in aqueous solution. The blue and red lines are the variations of the coordination numbers for the CV1 (C1–H, blue) and CV2 (C2–H, red).

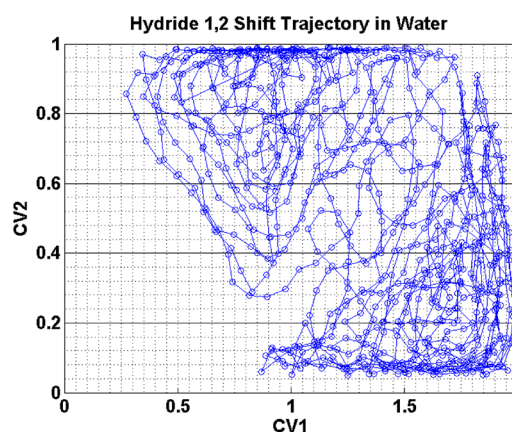
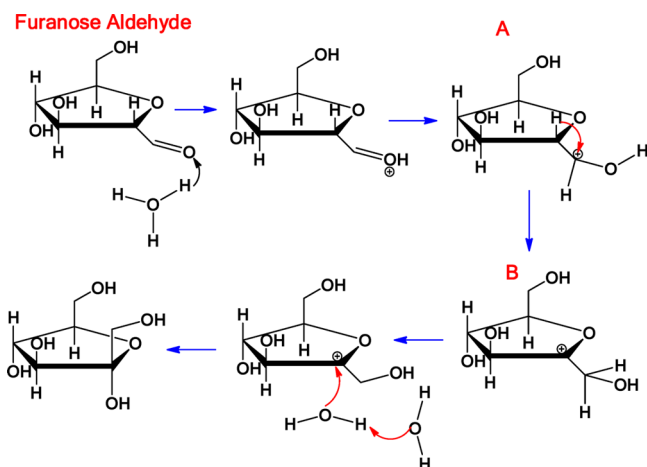


**Figure 6.** CV trajectories for CV1 (C1–H) and CV2 (C2–H) during the course of CPMD-MTD sampling process for hydride transfer from C2 to C1 in aqueous solution.

whereas CV2 fluctuates and decreases from 1 to 0.1 during the same period. This indicates a hydride has transferred from C1 to C2. At about 400 MTD step, both CV1 and CV2 are observed to restore to their starting values indicating both the reactant and product wells are filled and the FES becomes flat. Both CV1 and CV2 go back and forth rapidly during subsequent sampling from 400 to 900 MTD steps. The sampling appears to be complete during the 900 MTD steps of simulations.

During the course of CPMD-MTD sampling process for hydride transfer, the presence of solvent water molecules affects the reaction and associated energies dramatically. At the start of the simulations, the water molecule was seen to take away the proton from the C1 carbocation  $\text{—C1H}^+$  on the furanose intermediate A. Subsequently a neutral furanose aldehyde is formed. Further dehydration of this furanose aldehyde leads to the formation of HMF as shown in Scheme 1. Scheme 3 shows that besides dehydration to form HMF, competing reaction of hydride transfer from C2 on the furanose aldehyde to C1 leads to the isomerization to fructose. During this process, a proton is transferred from the neighboring  $\text{H}_3\text{O}^+$  in water to the aldehyde group  $\text{—C1H=O}$  to form  $\text{—C1H=O}^+\text{H}$  on the intermediate. The H atom on C2–H is subsequently transferred to the C1 atom to form  $\text{—CH}_2\text{—OH}$  resulting a furanose intermediate B with the carbocation on C2. As mentioned, before hydride transfer, the proton on  $\text{—C1H—OH}^+$  from intermediate A is transferred to the neighboring  $\text{H}_2\text{O}$  molecule to form  $\text{—C1H=O}$ . During the hydride transfer from C2 to C1, a proton from the  $\text{H}_3\text{O}^+$  in water is

**Scheme 3. Schematics for Hydride 1,2 Shift on Glucose Intermediate Furanose Aldehyde and the Subsequent Hydration of C2 Carbocation to Form Fructose during Acid-Catalyzed Glucose Isomerization to Fructose in Aqueous Solution**



subsequently transferred back to  $\text{-C1H=O}$  to form  $\text{-C1H}_2\text{-OH}$  with the positive charge shifted from C1 to C2 to form intermediate B. The total number of atoms on intermediate A and B before and after hydride transfer is conserved.

The energetics for the hydride transfer in water also changes significantly compared to those for the gas phase. Since the furanose aldehyde is much more stable than the positively charged furanose intermediate A, the associated barrier for hydride transfer from C2 to C1 is significantly higher than that in the gas phase. Figures 7 and 8 show the free energy contour

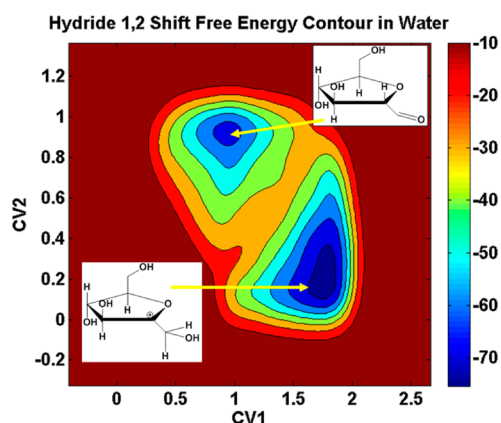


**Figure 7.** Free energy surface contour plot for hydride transfer in aqueous solution from C2 to C1 on the five-member ring intermediate during glucose isomerization reaction to form fructose via the cyclic mechanism initiated by protonation of C2-OH.

and reconstructed 3-D FES plots respectively. The initial structure of furanose aldehyde is located at  $\text{CV1} \approx 1$  and  $\text{CV2} \approx 0.9$  and the final structure after the hydride transfer from C2 to C1 is located at  $\text{CV1} \approx 1.8$  and  $\text{CV2} \approx 0.1$ . The barrier for the hydride 1,2 shift increases to about 35 kcal/mol in aqueous solution compared to 5–7 kcal/mol in the gas phase. This increase in the reaction barrier is due again to the solvent water molecule's high affinity to proton.  $\text{H}_2\text{O}$  can donate or remove proton from the reactive sugar molecule to stabilize the reactive intermediate. The free energy after the hydride transfer is about

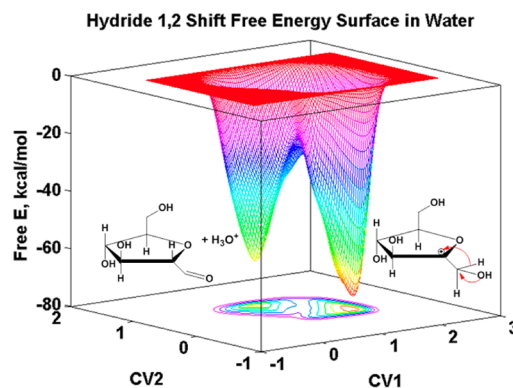


**Figure 8.** Reconstructed 3-D FES for CV1 (C1-H) and CV2 (C2-H) representing hydride transfer from C2 to C1 process in aqueous solution during glucose to fructose isomerization via the direct cyclic mechanism initiated by protonation of C2-OH.

10 kcal/mol lower than that before hydride transfer indicating that hydride 1,2 shift is a favorable process in the aqueous solution. Since the barrier associated with hydride 1,2 shift is about the same as or slightly higher than the first step in glucose dehydration reaction which has a barrier at around 30–35 kcal/mol,<sup>20</sup> glucose isomerization to fructose will be energetically difficult. This also explains why fructose from proton-catalyzed glucose isomerization has typically low yield in aqueous solutions. HMF formation is more favored due probably to the lower barrier associated with the dehydration process of removing two additional water molecules on the furanose aldehyde in the acidic environment.<sup>42,43</sup> We plan to further investigate the dehydration reaction from the furanose aldehyde to form HMF and compare the energetics obtained from glucose isomerization to fructose with hydride 1,2 shift process.

The hydride transfer from C2 to C1 creates a C2 carbocation. In the presence of solvent water molecules, the  $\text{H}_2\text{O}$  molecule could attack the C2 carbocation to form a C2-OH bond and generate furanose fructose molecule as shown earlier in Scheme 3. In an acidic environment, excess proton can be readily removed from the  $\text{C2}^+\text{-OH}_2$  by the solvent water molecule to form a  $\text{H}_3\text{O}^+$ . In order to quantify the energetics associated with this process, CPMD-MTD simulations were conducted for this fructose formation process starting with the C2 carbocation after the hydride transfer. Two CVs are used to describe this fructose reformation process. CV1 characterizes the CN of the O-H bond for the targeted water molecule during the nucleophilic attack. Before the reaction, CV1 is close to 2 since there are two H atoms associated with the O atom in the neutral water molecule. Once the C2-OH<sub>2</sub> bond forms, one proton will be removed by another neighboring water molecule to generate C2-OH and one  $\text{H}_3\text{O}^+$ . Once the proton is removed, CV1 is expected to be reduced to 1. CV2 characterizes CN for the C2-O bond. Before the reaction, CV2 is close to 0 indicating there is no direct bonding. Once the C2-OH is formed, CV2 reaches close to 1.

Figures 9 and 10 are the variations of the CN numbers and the trajectories of the two CVs during the course of the simulations. The formation of the C2-OH bond occurred after about 70 MTD simulation steps. However, the proton on the targeted water molecule was seen transferred back and forth between the O2H and the neighboring water molecule. The

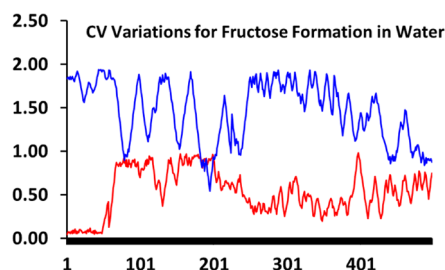


**Figure 9.** CV variations for fructose generation via rehydration of the C2 carbocation on furanose intermediate **B** after hydride 1,2 shift in aqueous solution. The blue and red lines are the variations of the coordination numbers for the CV1 (O2–H) and CV2 (C2–O).

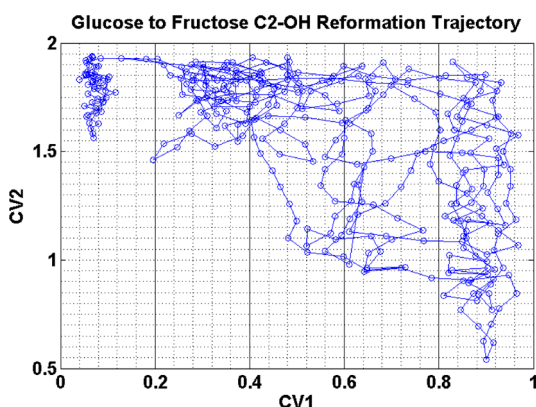


**Figure 10.** CV trajectories for CV1 (O2–H) and CV2 (C2–O) during the course of CPMD-MTD sampling process for hydration of C2 carbocation on furanose intermediate **B** during fructose generation in aqueous solution.

sampling of the final structure appears to be not complete due to the existence of possible several metastable structures besides fructose. The existence of an excess proton in the solution makes fructose potentially unstable. Nevertheless, the barrier for the cross over from the initial structure to the product well is generally valid and reliable.<sup>44</sup> Figures 11 and 12 are the free energy contour plot and the reconstructed 3-D free energy surface plot respectively associated with the fructose reformation process. It can be seen that, the initial structure of the C2 carbocation is located at CV1  $\approx$  0.1 and CV2  $\approx$  1.8 on the FES.

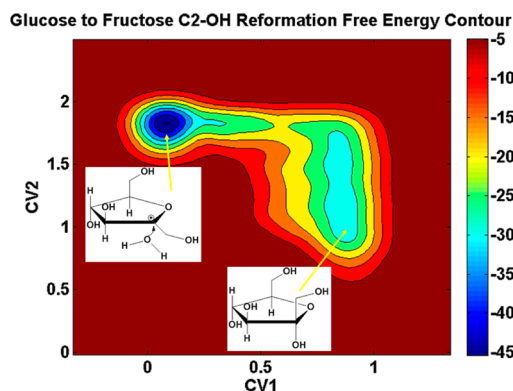


**Figure 11.** Free energy contour plot for fructose generation in aqueous solution during the reformation of C2–OH after hydride 1,2 shift from furanose aldehyde intermediate during glucose isomerization to fructose.

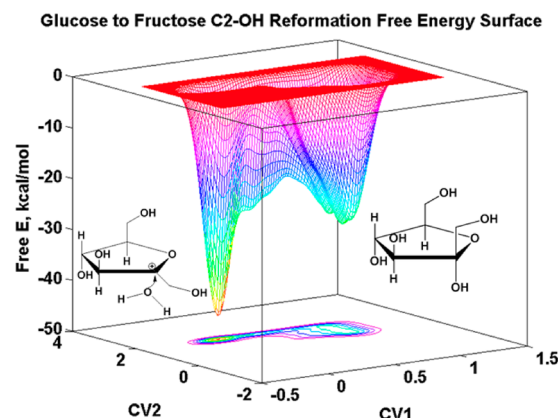


**Figure 12.** 3-D reconstructed free energy surface for fructose generation in aqueous solution during the reformation of C2–OH after hydride 1,2 shift on the furanose aldehyde intermediate during glucose isomerization to fructose.

The reformed fructose is located at CV1  $\approx$  0.8 and CV2  $\approx$  1. The barrier for forming the C2–OH bond is about 25 kcal/mol. This barrier is smaller than the barrier associated with hydride transfer in aqueous solution.

#### IV. CONCLUSIONS

Car–Parrinello ab initio molecular dynamics simulations (CPMD) coupled with metadynamics (MTD) simulations were conducted to investigate the glucose isomerization to fructose reaction in acidic aqueous solution. Glucose to fructose isomerization is initiated by protonation of the C2–OH and the formation of a furanose aldehyde intermediate. This furanose aldehyde is also the intermediate to produce HMF, a critical and versatile intermediate for biomass conversion to biofuel and biobased products. Fructose is produced via a hydride transfer from C2 to C1 on the furanose aldehyde followed by the rehydration of the C2 carbocation. This hydride 1,2 shift to form a C2 carbocation is an energetically favorable process but the barrier is relatively high at around 35 kcal/mol. Fructose is produced by the rehydration of the C2 carbocation with an estimated barrier of 25 kcal/mol from our CPMD-MTD simulations.

#### AUTHOR INFORMATION

##### Corresponding Author

\*E-mail: xqian@uark.edu.

##### Notes

The authors declare no competing financial interest.

#### ACKNOWLEDGMENTS

This work is supported by the NSF CAREER (CBET 0844882 and CBET 1137795). Calculations were carried out at High Performance Computing Center (HPC) from the University of Arkansas and Teragrid.

#### REFERENCES

- (1) Brown, D. W.; Floyd, A. J.; Kinsman, R. G.; Roshanali, Y. *J. Chem. Technol. Biotechnol.* **1982**, 32, 920–924.
- (2) Roman-Leshkov, Y.; Chhedha, J. N.; Dumesic, J. A. *Science* **2006**, 312, 1933–1937.
- (3) van Damm, H. E.; Kieboom, A. P. G.; van Bekkum, H. *Starch* **1986**, 38, 95–101.
- (4) Musau, R. M.; Munavu, R. M. *Biomass* **1987**, 13, 67–74.



- (5) Szmant, H. H.; Chundury, D. D. *J. Chem. Technol. Biotechnol.* **1981**, *31*, 135–145.
- (6) Nakamura, Y.; Morikawa, S. *Bull. Chem. Soc. Jpn.* **1980**, *53*, 3705–3706.
- (7) Zhao, H. B.; Holladay, J. E.; Brown, H.; Zhang, Z. C. *Science* **2007**, *316*, 1597–1600.
- (8) Qian, X. H.; Nimlos, M. R.; Johnson, D. K.; Himmel, M. E. *Appl. Biochem. Biotechnol.* **2005**, *121*, 989–997.
- (9) Qian, X. H.; Nimlos, M. R.; Davis, M.; Johnson, D. K.; Himmel, M. E. *Carbohydr. Res.* **2005**, *340*, 2319–2327.
- (10) Bicker, M.; Hirth, J.; Vogel, H. *Green Chem.* **2003**, *5*, 280–284.
- (11) Chheda, J. N.; Roman-Leshkov, Y.; Dumesic, J. A. *Green Chem.* **2007**, *9*, 342–350.
- (12) Chheda, J. N.; Huber, G. W.; Dumesic, J. A. *Angew. Chem., Int. Ed.* **2007**, *46*, 7164–7183.
- (13) Chheda, J. N.; Dumesic, J. A. *Catal. Today* **2007**, *123*, 59–70.
- (14) Seri, K.; Inoue, Y.; Ishida, H. *Bull. Chem. Soc. Jpn.* **2001**, *74*, 1145–1150.
- (15) Kuster, B. F. M. *Starch/Staerke* **1990**, *42*, 314–321.
- (16) Chheda, J. N.; Barrett, C. J.; Huber, G. W.; Dumesic, J. A. *Abs. Am. Chem. Soc.* **2006**, *231*, 1.
- (17) Zhang, Y. T.; Du, H. B.; Qian, X. H.; Chen, E. Y. X. *Energy Fuels* **2010**, *24*, 2410–2417.
- (18) Du, H. B.; Qian, X. H. *Carbohydr. Res.* **2011**, *346*, 1985–1990.
- (19) Liu, D. J.; Nimlos, M. R.; Johnson, D. K.; Himmel, M. E.; Qian, X. H. *J. Phys. Chem. A* **2010**, *114*, 12936–12944.
- (20) Qian, X. H. *J. Phys. Chem. A* **2011**, *115*, 11740–11748. Qian, X. H. *Top. Catal.* **2012**, *55*, 218–226.
- (21) Qian, X. H.; Johnson, D. K.; Himmel, M. E.; Nimlos, M. R. *Carbohydr. Res.* **2010**, *345*, 1945–1951.
- (22) Dong, H.; Nimlos, M. R.; Himmel, M. E.; Johnson, D. K.; Qian, X. H. *J. Phys. Chem. A* **2009**, *113*, 8577–8585.
- (23) Antal, M. J.; Mok, W. S. L.; Richards, G. N. *Carbohydr. Res.* **1990**, *199*, 91–109.
- (24) Feather, M. S. *Tetra. Lett.* **1970**, *48*, 4143–4145.
- (25) Antal, M. J.; Leesomboon, T.; Mok, W. S.; Richards, G. N. *Carbohydr. Res.* **1991**, *217*, 71–85.
- (26) Feather, M. S.; Harris, D. W.; Nichols, S. B. *J. Org. Chem.* **1972**, *37*, 1606–1608.
- (27) Feather, M. S.; Harris, J. F. *Carbohydr. Res.* **1970**, *15*, 304–309.
- (28) Qian, X.; Nimlos, M. R. In *Biomass Recalcitrance*; Himmel, M., Ed.; Blackwell Publishing Ltd.: Oxford, U.K., 2008; pp 331–349.
- (29) Harris, D. W.; Feather, M. S. *J. Org. Chem.* **1974**, *39*, 724–725.
- (30) Laio, A.; Parrinello, M. *Proc. Natl. Acad. Sci. U.S.A.* **2002**, *99*, 12562–12566.
- (31) Iannuzzi, M.; Laio, A.; Parrinello, M. *Phys. Rev. Lett.* **2003**, *90*, 238302.
- (32) Car, R.; Parrinello, M. *Phys. Rev. Lett.* **1985**, *55*, 2471–2474.
- (33) Andersen, H. C. *J. Chem. Phys.* **1980**, *72*, 2384–2393.
- (34) Nose, S. *Mol. Phys.* **1984**, *52*, 255–268.
- (35) Becke, A. D. *Phys. Rev. A* **1988**, *38*, 3098.
- (36) Lee, C.; Yang, W.; Parr, R. G. *Phys. Rev. B* **1988**, *37*, 785.
- (37) Goedecker, S.; Teter, M.; Hutter, J. *Phys. Rev. B* **1996**, *54*, 1703–1710.
- (38) Nose, S. *J. Chem. Phys.* **1984**, *81*, 511.
- (39) Hoover, W. G. *Phys. Rev. A* **1985**, *31*, 1695.
- (40) Tuckerman, M. E.; Parrinello, M. *J. Chem. Phys.* **1994**, *101*, 1302–1315.
- (41) Hockney, R. W. *Methods Comput. Phys.* **1970**, *9*, 136.
- (42) Nimlos, M. R.; Blanksby, S. J.; Qian, X. H.; Himmel, M. E.; Johnson, D. K. *J. Phys. Chem. A* **2006**, *110*, 6145–6156.
- (43) Nimlos, M. R.; Qian, X. H.; Davis, M.; Himmel, M. E.; Johnson, D. K. *J. Phys. Chem. A* **2006**, *110*, 11824–11838.
- (44) Laio, A.; Rodriguez-Forte, A.; Gervasio, F. L.; Ceccarelli, M.; Parrinello, M. *J. Phys. Chem. B* **2005**, *109*, 6714–6721.